Supplement of Atmos. Chem. Phys. Discuss., 15, 32967–33002, 2015
http://www.atmos-chem-phys-discuss.net/15/32967/2015/
doi:10.5194/acpd-15-32967-2015-supplement

Supplement of

Effect of varying experimental conditions on the viscosity of α-pinene derived secondary organic material

J. W. Grayson et al.

Correspondence to: A. K. Bertram (bertram@chem.ubc.ca)

1 Effect of carrier gas flow on SOM particle properties

To determine whether particles evaporate whilst being exposed to a flow of N_2 gas, a sample (generated with a mass concentration of 6,000 μg m^{-3}) was mounted in the flow cell and exposed to dry (<0.5 % RH) N_2 gas for a period of 45 h. A series of nine images were taken of each of five particles over a time period of 45 h. The area at the particle-substrate interface of each particle was measured using Leica software, and equilibrium contact angle measurements of particles in the sample were made after the completion of the experiment. From this information, the volume of each of the particles was determined at each time point, with the equilibrium contact angle assumed to remain constant during the duration of the experiment. To remove the potential of photo-induced changes to the sample the light source was only turned on when acquiring images. Poke-flow experiments were also performed after 1 h and 45 h of exposure to the dry N_2 gas flow to determine whether the viscosity of the particles changed due to the extended exposure. The results of these studies are shown in Figure S1 and Table S1.

2 Variability between particles in the same sample, and between all particles produced under equivalent conditions

To determine the variability in $\tau_{exp,flow}$ and the variability in the simulated lower and upper limits of viscosity for particles produced using equivalent conditions, the percent relative standard deviations (% RSD) have been calculated for poke-flow experiments performed at <0.5 % RH, and are reported in Table S4.

Table S4 shows the % RSD for all particles produced under equivalent conditions ranged from 26-117 %. For samples on the same substrate, the % RSD ranged from 14-83 %. In general there appears to be a reasonable level of reproducibility in results both between particles on the same substrate, and between particles on separate substrates produced under equivalent conditions. The majority of the uncertainty in the reported viscosities is due to uncertainty in the physical parameters used during simulations, rather than experimental variability or error, as can be seen in Figs. 3b, 5b, & S3b.

3 Calculation of limits of viscosity from previous studies of SOM produced via the ozonolysis of α-pinene

Saleh et al. (2013) and Robinson et al. (2013) reported mixing times for particles of a given size, which have been used to calculate diffusion coefficients through the relationship,

$$D = d_p^2/4\pi^2\tau_{mixing} \tag{1}$$

where d$_p$ is the diameter of the particle (m), and τ_{mixing} is the mixing time in s (Shiraiwa et al., 2011). The calculated diffusion coefficients for Saleh et al. (2013) and Robinson et al. (2013) should be considered as lower limits, as the mixing times used were the upper limit of those reported, and other processes besides molecular diffusion within the particles may have been the rate determining step for mixing in their experiments. These calculated upper limits to diffusion coefficients were then converted to lower limits of viscosities through the Stokes-Einstein relationship,

$$\mu = kT/x\pi rD \tag{2}$$

where k is the Boltzmann constant (J K^{-1}), T is the temperature (K), x is a coefficient ranging from 4-6 dependent upon the assumption of slip or no-slip at the surface of the diffusing species, and r is the hydrodynamic radius of the diffusing molecule (m). A summary of the values used to calculate viscosities is included in Table S5.

As the size of the diffusing molecules were not known in Saleh et al. (2013) and Robinson et al. (2013), we assumed a hydrodynamic radius of 0.38 nm, which corresponding to the radii of a symmetrically spherical molecule of molar mass 175 g mol^{-1} (Huff-Hartz, 2005) and density 1.3 g cm^{-3} (Chen and Hopke, 2009). Further, x has been given a value of 4, to give conservative upper limits to viscosity.

Abramson et al. (2013) determined the diffusion coefficient for pyrene molecules in particles of SOM generated via the ozonolysis of α-pinene. The hydrodynamic radius of pyrene is 0.4 nm, whilst, as suggested by Abramson et al. (2013) pyrene may form clusters consisting of up to 1000 molecules, with a 1000 molecule cluster having a radius of $\approx$4 nm. Hence, when calculating viscosity using Equation S2, from the studies of Abramson et al., we used r = 0.4 to 4 nm. Further, we used x = 4-6 in Equation 2 to calculate conservative lower and upper limits of viscosity.

Cappa and Wilson (2011) observed the change in chemical composition of SOM particles produced via the ozonolysis of α-pinene as the particles were heated, and conservatively estimated an upper limit of diffusion coefficient for the particles. A value of x = 6 has been used in Equation S2, along with a value of r = 4 nm, in order to determine a lower limit of viscosity.

Perraud et al. (2012) studied the particulate nitrate concentration in SOM particles generated via the ozonolysis of α-pinene and determined an upper limit for the diffusion coefficient of the particles. A value of x = 6 has been used in Equation S2, along with a value for r of 4 nm, in order to determine a lower limit of viscosity.

4 Studies using the poke-and-flow technique combined with simulations of fluid flow for particles that exhibited cracking behaviour

In some cases (for the water-soluble SOM at low RH) the needle did not penetrate the particle. Instead, the needle caused the particle to ’crack’, resulting in sharp, defined edges in the SOM (see Figure 6, panel b2 for an example). In cases where cracking occurred, the material was observed for an extended period of time (at least 12 h). If, over that time, the sharp, defined, edges exhibited no detectable movement, the observation time was taken as a lower limit of $\tau_{exp,flow}$.

Particles that exhibited cracking behaviour and no detectable flow over the course of an experiment were simulated using a particle of quarter-sphere geometry, with one flat surface in contact with a solid substrate (see Figure S4b and Movie S5 in Renbaum-Wolff et al. (2013)). The bottom surface, which represented the material-substrate interface, was allowed to undergo free deformation in the horizontal plane. All other surfaces were allowed to undergo free deformation in all directions. In these simulations the viscosity of the particle was varied until the sharp edge at the top of the particle moved by 0.5 μm over the experimental time. A value of 0.5 μm was chosen because this amount of movement is a clearly detectable threshold for the microscopy. Thus, for experiments for which no detectable movement was observed in microscope images, the viscosity determined via this method is a lower limit. The values of density, particle-substrate slip length, surface tension, and contact angle used when simulating the lower limit of viscosity for these particles are detailed in Table S6.

References

Abramson, E., Imre, D., Beránek, J., Wilson, J., and Zelenyuk, A.: Experimental determination of chemical diffusion within secondary organic aerosol particles., Physical Chemistry Chemical Physics, 15, 2983–2991, doi:10.1039/c2cp44013j, 2013.

Cappa, C. D. and Wilson, K. R.: Evolution of organic aerosol mass spectra upon heating: implications for OA phase and partitioning behavior, Atmos. Chem. Phys., 11, 1895–1911, doi:10.5194/acp-11-1895-2011, 2011.

Chen, X. and Hopke, P. K.: Secondary organic aerosol from α-pinene ozonolysis in dynamic chamber system, Indoor air, 19, 335–345, doi:10.1111/j.1600-0668.2009.00596.x, 2009.

Grayson, J. W., Song, M., Sellier, M., and Bertram, A. K.: Validation of the poke-flow technique combined with simulations of fluid flow for determining viscosities in samples with small volumes and high viscosities, Atmos. Meas. Tech., 8, 2463–2472, doi:10.5194/amtd-8-877-2015, 2015.

Huff-Hartz, K. E.: Cloud condensation nuclei activation of monoterpene and sesquiterpene secondary organic aerosol, Journal of Geophysical Research, 110, D14 208, doi:10.1029/2004JD005754, 2005.

Perraud, V., Bruns, E. A., Ezell, M. J., Johnson, S. N., Yu, Y., Alexander, M. L., Zelenyuk, A., Imre, D., Chang, W. L., Dabdub, D., Pankow, J. F., and Finlayson-Pitts, B. J.: Nonequilibrium atmospheric secondary organic aerosol formation and growth., Proceedings of the National Academy of Sciences of the United States of America, 109, 2836–2841, doi:10.1073/pnas.1119909109, http://www.ncbi.nlm.nih.gov/pmc/articles/PMC3286997/, 2012.

Renbaum-Wolff, L., Grayson, J. W., Bateman, A. P., Kuwata, M., Sellier, M., Murray, B. J., Shilling, J. E., Martin, S. T., and Bertram, A. K.: Viscosity of α-pinene secondary organic material and implications for particle growth and reactivity., Proceedings of the National Academy of Sciences of the United States of America, 110, 8014–8019, doi:10.1073/pnas.1219548110, http://www.ncbi.nlm.nih.gov/pmc/articles/PMC3657821/, 2013.

Robinson, E. S., Saleh, R., and Donahue, N. M.: Organic aerosol mixing observed by single-particle mass spectrometry., The Journal of Physical Chemistry A, 117, 13 935–13 945, doi:10.1021/jp405789t, 2013.

Saleh, R., Donahue, N. M., and Robinson, A. L.: Time scales for gas-particle partitioning equilibration of secondary organic aerosol formed from alpha-pinene ozonolysis., Environmental Science & Technology, 47, 5588–5594, doi:10.1021/es400078d, 2013.

Shiraiwa, M., Ammann, M., Koop, T., and Pöschl, U.: Gas uptake and chemical aging of semisolid organic aerosol particles., Proceedings of the National Academy of Sciences of the United States of America, 108, 11 003–11 008, doi:10.1073/pnas.1103045108, http://www.ncbi.nlm.nih.gov/pmc/articles/PMC3131339/, 2011.

Tuckermann, R. and Cammenga, H. K.: The surface tension of aqueous solutions of some atmospheric water-soluble organic compounds, Atmospheric Environment, 38, 6135–6138, 2004.

Zhang, Y., Sanchez, M. S., Douet, C., Wang, Y., Bateman, A. P., Gong, Z., Kuwata, M., Renbaum-Wolff, L., Sato, B. B., Liu, P. F., Bertram, A. K., Geiger, F. M., and Martin, S. T.: Changing shapes and implied viscosities of suspended submicron particles, Atmos. Chem. Phys., 15, 7819–7829, doi:10.5194/acpd-15-7783-2015, 2015.

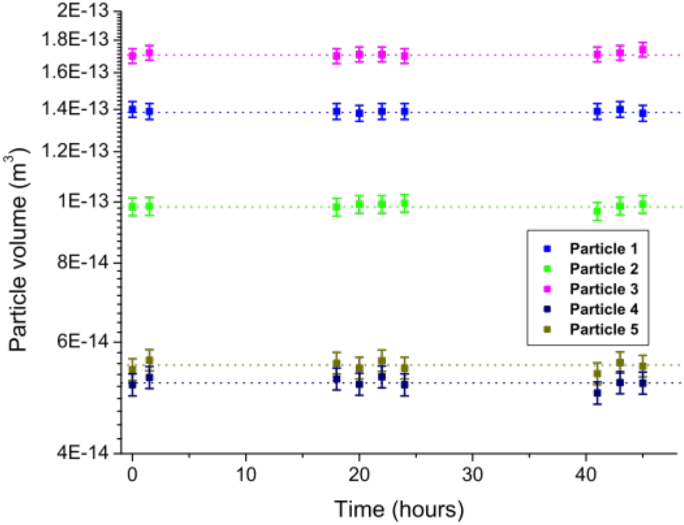

Figure 1. A plot of particle volume vs. time for five particles exposed to a dry (<0.5 % RH) N_2 gas flow. Dotted lines represent the measured mean size of a particle. Error bars on the y-axis represent the uncertainty in measuring both the area of the particle, and the equilibrium contact angle, at the particle-substrate interface.

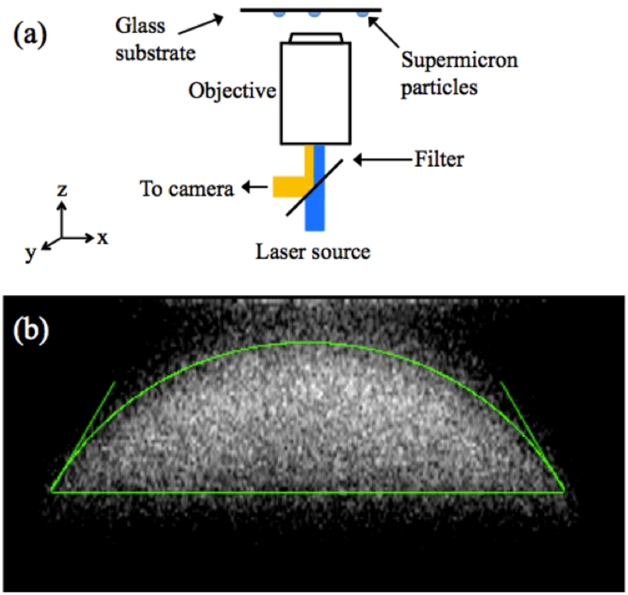

Figure 2. (a) Schematic representation of instrumental setup for contact angle images. (b) Fluorescence image obtained of an SOM particle. The green overlay is used to determine the contact angle of the particle, in this case 60^0, and was produced using the LB-ADSA plugin for ImageJ.

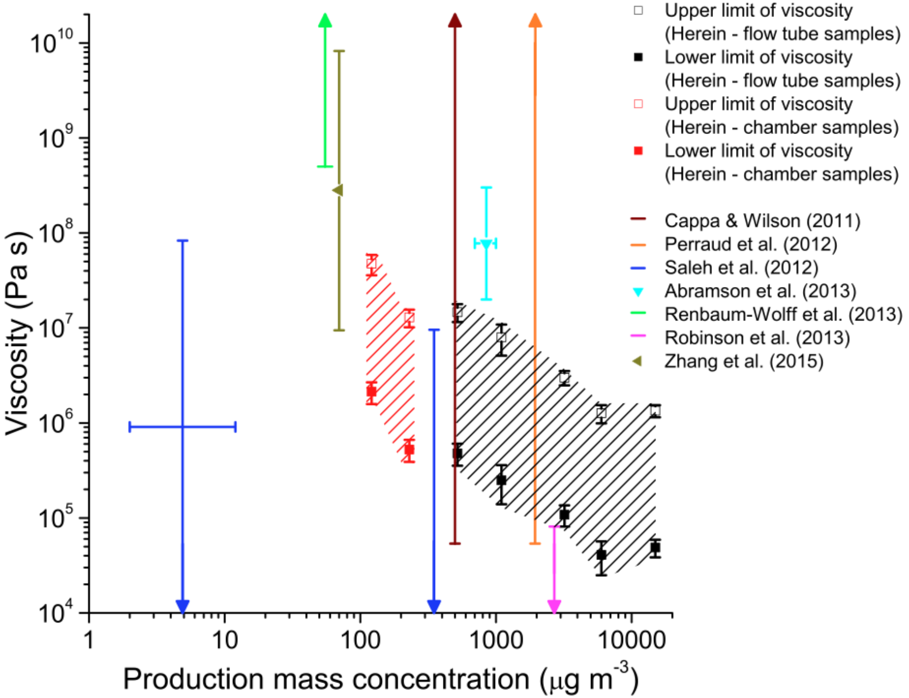

Figure 3. Plot of production mass concentration vs. viscosity for whole SOM produced via the ozonolysis of α-pinene and studied at <5 % RH. Shown are the results determined here along with those previously reported in literature (Cappa and Wilson, 2011; Perraud et al., 2012; Saleh et al., 2013; Abramson et al., 2013; Renbaum-Wolff et al., 2013; Robinson et al., 2013; Zhang et al., 2015).

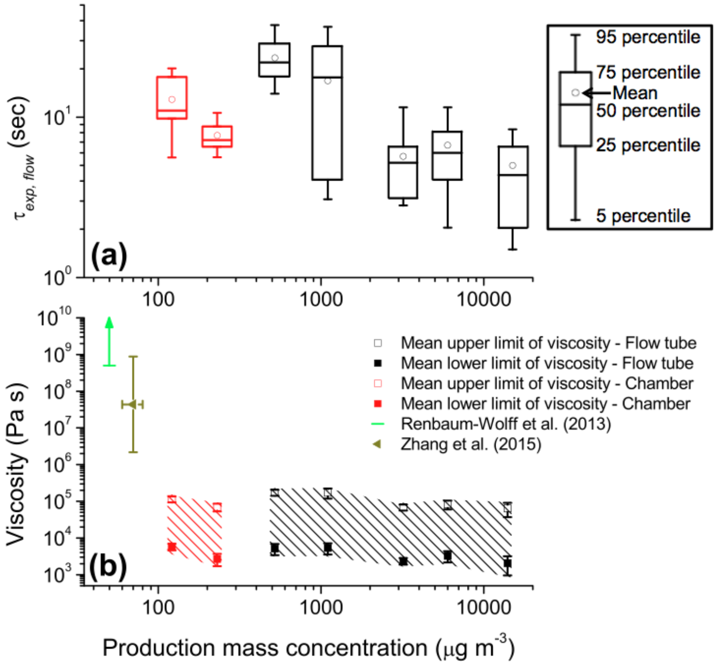

Figure 4. Summary of poke-flow experiments performed on particles of whole SOM at 30 % RH. Black symbols represent results from particles produced in a flow tube, whilst red symbols represent results from particles produced in a chamber. Panel (a) shows box plots of observed $\tau_{exp,flow}$ times at different SOM mass concentrations for particles studied using the poke-and-flow at 30 % RH. Boxes represent the 25, 50, and 75 percentiles, open circles represent median values, and whiskers represent the 5 and 95 percentiles. Panel (b) shows the simulated lower (filled squares) and upper (open squares) limit of viscosity for particles at each SOM mass concentration studied using the poke-and-flow technique at 30 % RH. Symbols represent mean values, whilst the y error bars represent 95 % confidence intervals. The shaded region is included to guide the eye of the reader. Also included in (b) are literature viscosities from Renbaum-Wolff et al. (2013) and Zhang et al. (2015), for SOM produced via the ozonolysis of α-pinene and studied at 30 % RH.

Table 1. Summary of $\tau_{exp,flow}$ times and viscosities of sample analysed after both 1 hour and 45 hours of exposure to a dry (<0.5 % RH) flow of Nitrogen gas.

Exposure time	$\tau_{exp,flow}$ (sec) [a]	Mean simulated viscosity ± 95 % confidence intervals (Pa s) [b]	
		Lower limit	Upper limit
1 hour	104.3 (80.3,120.5)	$1.5 \times 10^4 \pm 5.0 \times 10^3$	$6.4 \times 10^5 \pm 9.0 \times 10^4$
45 hours	107.8 (80.6, 141.1)	$3.0 \times 10^4 \pm 9.3 \times 10^3$	$1.0 \times 10^6 \pm 2.3 \times 10^5$

[a] $\tau_{exp,flow}$ values represent experimental values in the form "mean (5th percentile, 95th percentile)".

Table 2. Physical parameters used when simulating particles that exhibited flow with COMSOL.

	Density (kg m^{-3}) [a]	Slip length (m) [b]	Surface tension (mN m^{-1}) [c]	Contact angle
Value used to determine lower limit of viscosity	1,300	5×10^{-9}	40	See Table S3 [d]
Value used to determine upper limit of viscosity	1,300	1×10^{-5}	75	See Table S3 [d]

[a] Density was varied from 1,000 - 1,400 kg m^{-3} based on the work of Chen and Hopke (2009) and determined to have no effect upon viscosities determined via simulation. As such a median value of 1300 kg m^{-3} was used.

[b] For references and rationale see Grayson et al. (2015).

[c] Range of surface tension values based on work on Tuckermann and Cammenga (2004).

[d] The lower value from Table S3 is used for particles of geometry (R_0 - r_0) / r_0 <2, and the upper value from Table S3 is used for particles of geometry (R_0 - r_0) / r_0 >2.

[e] The upper value from Table S3 is used for particles of geometry (R_0 - r_0) / r_0 <2, and the lower value from Table S3 is used for particles of geometry (R_0 - r_0) / r_0 >2.

Table 3. Experimentally determined contact angles for each of the samples studied. The range of values represent the 95 % confidence intervals of the values measured for multiple particles.

Sample name (production mass concentration during SOM production)	Particle-substrate contact angle (^{0})		
	Sample 1	Sample 2	Sample 3
Water-soluble SOM (14,000 μg m^{-3})	43.5 - 50.0	47.2 - 53.3	50.5 - 72.0
Flow tube sample #1 (14,000 μg m^{-3})	57.5 - 63.7	49.6 - 55.4	18.3 - 21.4
Flow tube sample #2 (6,000 μg m^{-3})	59.8 - 61.3	60.5 - 66.9	63.3 - 67.2
Flow tube sample #3 (3,200 μg m^{-3})	41.2 - 52.2	38.5 - 45.3	49.2 - 51.1
Flow tube sample #4 (1,100 μg m^{-3})	31.4 - 35.6	61.5 - 65.5	44.3 - 47.8
Flow tube sample #5 (520 μg m^{-3})	55.5 - 61.8	56.2 - 60.6	36.1 - 47.0
Chamber sample #1 (230 μg m^{-3})	64.5 - 69.0	64.1 - 66.5	
Chamber sample #2 (121 μg m^{-3})	60.2 - 65.1	60.7 - 80.1	

Table 4. Summary of the percent relative standard deviation (% RSD) in $\tau_{exp,flow}$, lower limits of viscosity, and upper limits of viscosity for particles produced using equivalent conditions and studied via the poke-flow technique in combination with simulations of fluid flow at <0.5 % RH. Three samples were studied per production mass concentration in the flow tube. Values prior to parentheses represent the relative standard deviation between all particles studied that were produced at a given mass concentration, whilst the values inside each parenthesis represent the average relative standard deviation between particles on the same substrate.

SOM mass particle concentration (μg m^{-3})	% RSD of $\tau_{exp,flow}$	% RSD of simulated lower limit of viscosity	% RSD of simulated upper limit of viscosity
520	54 (30)	68 (67)	56 (39)
1,100	89 (24)	117 (44)	96 (27)
3,200	27 (22)	67 (42)	45 (30)
6,000	26 (20)	103 (47)	58 (29)
14,000	31 (27)	57 (27)	40 (28)

Table 5. Summary of parameters used to estimate viscosity from literature studies of SOM produced via the ozonolysis of α-pinene.

Reference	d_p (nm)	τ_{mixing} (sec)	x	r (nm)
Cappa and Wilson (2011)	N/A		6	4.0
Perraud et al. (2012)	N/A		6	4.0
Saleh et al. (2013) [a]	112 [b]	3,600	4	0.38
Saleh et al. (2013) [c]	38 [b]	3,600	4	0.38
Abramson et al. (2013)	N/A		4 - 6	0.4 - 4.0
Robinson et al. (2013)	>158 [b]	60	4	0.38

[a] Values for experiments conducted with an SOM mass concentration of 350 μg m^{-3}.

[b] An aerodynamic diameter was reported, and has been converted to a geometric diameter here.

[c] Values for experiments conducted with an SOM mass concentration of 1-12 μg m^{-3}.

Table 6. Physical parameters when simulating particles that don't exhibit flow in COMSOL

	Density (kg m^{-3}) [a]	Slip length (m) [b]	Surface tension (mN m^{-1}) [c]	Contact angle (^{0})
Value used to determine lower limit of viscosity	1,300	1 - 1.7 x 10^{-8}	40	90

[a] Density was varied from 1,000 - 1,400 kg m^{-3} based on the work of Chen and Hopke (2009) and determined to have no effect upon simulations values. As such a median value of 1300 kg m^{-3} was used.

[b] For references and rationale see Grayson et al. (2015).

[c] Surface tension value based on work on Tuckermann and Cammenga (2004).